Electric Power Systems Research 212 (2022) 108533

Contents lists available at ScienceDirect

Electric Power Systems Research

journal homepage: www.elsevier.com/locate/epsr

Optimizing system operation with nadir considerations via simulations of detailed system dynamic responses

Diego Ortiz-Villalba [a,*], Jacqueline Llanos [a], Yanira Muñoz-Jadan [b], Rodrigo Moreno [b,c,d], Claudia Rahmann [b], Bikash C. Pal [c]

[a] Department of Electrical and Electronic Engineering, Universidad de las Fuerzas Armadas ESPE, Sangolquí, Ecuador
[b] Department of Electrical Engineering, University of Chile, Santiago, Chile
[c] Department of Electrical and Electronic Engineering, Imperial College London, UK
[d] Instituto Sistemas Complejos de Ingeniería, Santiago, Chile

ARTICLE INFO

Keywords:
System inertia
Primary frequency response
Power imbalance
Governor ramp rate
Stability assessment

ABSTRACT

Decarbonization processes around the world are pressing system operation significantly, particularly in terms of ensuring appropriate reliability and stability levels when integrating massive amounts of converter-based generation technologies (CGTs). In this context, this work proposes an optimization-simulation model to optimize system operation with nadir considerations via simulation of detailed system dynamic responses. We propose a Gauss–Seidel iterative method to incorporate the precise governors' dynamic responses determined by the simulations within the sequential optimization problems. Through several case studies, we demonstrate the benefits of our approach and analyze the impacts of incorporating a detailed representation of units' dynamic responses. We also compare our frequency nadir-constrained approach against an alternative inertia-constrained approach that ensures minimum amounts of inertia levels. Particularly, we show that ensuring minimum amounts of inertia may lead to inefficient economic outputs in terms of costs and integration of renewable generation without security gains in terms of frequency stability compared with constraining frequency nadir.

1. Introduction

1.1. Motivation

In power systems dominated by synchronous generators (SG), the mechanical inertia needed to ensure the frequency response during major power imbalances has been traditionally provided by the rotating machines. Unlike conventional SG, converter-based generation technologies (CGTs) do not contribute with inertial response during major system imbalances. High penetration levels of CGTs lead to a reduction of the overall inertia of the system. Consequently, the system's ability to arrest frequency deviations during disturbances may be significantly affected and thus frequency stability. Hence, power system operational models (economic dispatch models, optimal power flow models, unit commitment models, etc.) need to consider new approaches to ensure system stability going forward, particularly in terms of frequency deviations.

The North American Electric Reliability Corporation (NERC) defines the primary frequency response (PFR) as the actions to arrest and stabilize frequency in response to frequency deviations [1]. PFR comes from SG (inertia) and load response. In addition, it can come from prime mover governors. In our work, PFR will be defined as to be adequate if system frequency does not droop below a given threshold after the disconnection of the largest online generating unit. The frequency response has an important influence on power system reliability, and one of the key challenges is maintaining the grid frequency within a specified limit. With the integration of more and more CGTs due to environmental concerns, the control of the power systems is becoming significantly more complex [2,3].

For instance, the quality of frequency control in the United States has been declined in recent years, requiring adequate planning of primary frequency control [4]. In the same vein, Britain's primary reserve requirements have increased due to the installed capacity of wind farms [5]. Ireland and Iowa have reported that the inertial response and PFR have been deteriorated due to the important levels of wind generation penetration [6,7]. In this context of environmental awareness and increased penetration of CGTs, advanced models are required to operate power systems in a reliable manner, particularly in terms of the needed means to control system frequency adequately.

* Corresponding author.
E-mail address: ddortiz5@espe.edu.ec (D. Ortiz-Villalba).

https://doi.org/10.1016/j.epsr.2022.108533
Received 3 October 2021; Received in revised form 17 April 2022; Accepted 2 July 2022
Available online 19 July 2022

Nomenclature

Sets

B	Set of nodes
I	Set of generating units
I_b	Set of indexes of generators connected to node b
K	Set of transmission lines

Parameters

c_i	Variable cost of generator i [$/MW]
D_b	Load in node b [MW]
f_{db}	Dead-band frequency [Hz]
$\overline{f_K}$	Capacity of line k [MW]
f_{min}	Minimum frequency [Hz]
f_{Nadir}	Nadir frequency [Hz]
$fr(k)$	Sending or origin node of line k
f_0	Nominal frequency [Hz]
M_i	Angular momentum of generator i [MWs/Hz]
$\overline{P_i}$	Capacity of generator i [MW]
$\underline{P_i}$	Minimum stable generation of generator i [MW]
P_ℓ	Largest power loss [MW]
$\overline{R_i}$	Maximum reserve from generator i [MW]
T_H	Requirement of system angular momentum [MWs/Hz]
$to(k)$	Receiving or destination node of line k
x_k	Reactance of line k [Ohms]
ρ_i	Governor response/ramp rate of generator i [MW/s]

Variables

f_k	Power flow of line k [MW]
M_H	Total angular momentum
P_i	Power output of generator i [MW]
R_i	Reserve provision of generator i [MW]
Y_i	Unit commitment variable (binary on/off)
θ_b	Phase angle in node b [rad]

1.2. Literature review

Optimal system operation (and planning) is determined through optimization models that, except for reserves requirements, usually ignore details associated with frequency excursion due to contingencies [8]. This, however, is changing due to the rapid deployment of CGTs. Hence, different approaches have been proposed lately in the literature to model the system frequency response within operational and planning models. For instance, planning models with frequency control have been proposed in [8,9], unit commitment (UC) models considering the frequency response have been presented in [10–12], and further power system operational models including detailed frequency security constraints have been proposed in [13–15].

A traditional generation expansion planning problem by considering flexibility and frequency security assessment is presented in [9]. The proposal formulates a two-stage optimization model. The first stage corresponds to the traditional resource planning problem, while the second stage aims to enhance flexibility to satisfy frequency security constraints.

In [8] a cost-risk model is proposed. The model includes the provision of various generation frequency control and demand-side services, including preservation of system inertia levels. The optimization problem considers a frequency nadir constraint that ensures a lower bound for the post-contingency frequency excursion.

A frequency-constrained stochastic unit commitment model is proposed in [10]. The model co-optimizes energy production along with the provision of synchronized and synthetic inertia, enhanced frequency response, primary frequency response, and other reserves services. Through linear approximations, the model is able to capture many details in terms of frequency control services and the demand/load response.

In [11] a security-constrained unit commitment (SCUC) problem is proposed, including frequency response. The proposal includes a technique to linearize the nonlinear function representing the minimum system frequency in order to include the security constraint related to the PFR in the optimization problem.

An algorithm that includes inertia and PFR requirements in the day-ahead UC problem is presented in [12]. The algorithm includes a simplified dynamic model to determine the frequency nadir in every hour of the UC. When the frequency drops under a threshold, the algorithm increases the spinning reserve and re-optimizes the UC, repeating the process until the frequency nadir is equal or above a threshold.

The authors in [13] propose a formulation of system strength and inertia-constrained generation dispatch to reassure operational security in the National Electricity Market (NEM) of Australia. An aggregated ramp rate in MW/s of the overall governor responses in the power system is assumed. The system strength contribution factor of an SG is defined to linearize the system strength constraint.

In [14], the authors propose a method to formulate linear frequency security constraints, which considers frequency response. Three methods are compared. Two of them consider that the generators increase their power with a constant governor ramp rate. In contrast, the third method simplifies the governor characteristic by a single aggregated governor. Then, an evaluation methodology is designed to quantify the accuracy of those frequency constraints.

In [15] an optimal power flow model is proposed to include primary frequency response and secondary frequency response requirements. A simplified governor turbine model is considered, where the governor ramp rate for each SG is defined as a constant.

There are several works in the technical literature related to optimal power system operation/planning models with frequency control and nadir considerations. However, it is hard to find models considering the differences in the dynamic response of each SG in terms of governor ramp rates. Indeed, most of the works assume a generic governor response equal across all SG. Importantly, the dynamic performance of power systems depends strongly on the particular characteristics of each SG; therefore, ignoring the differences among SG may lead to significant inaccuracies. In addition, a unit's governor ramp rate is not a constant, and it depends on its operating point. Our proposed model tackles these problems, considering, for a given contingency, the detailed inertial response of every unit according to its particular operating point, incorporating this information (iteratively) within the frequency-constrained optimization problem used that determines the optimal power system operation.

1.3. Proposition and contributions

We propose a two-stage optimization-simulation model to determine system operation, considering a system frequency nadir constraint. The optimization stage finds optimal solutions that comply with a system frequency nadir constraint against the loss of the largest unit; and the simulation stage determines the detailed system dynamic responses, which are iteratively incorporated within the optimization problem. The optimization and simulation stages are run iteratively as the detailed dynamic responses of generators change depending on the dispatch solution found by the optimization part.

Our modeling approach presents two distinctive characteristics. First, this is tractable to solve large-scale system operation (dispatch) problems, including co-optimization of energy and reserve services.

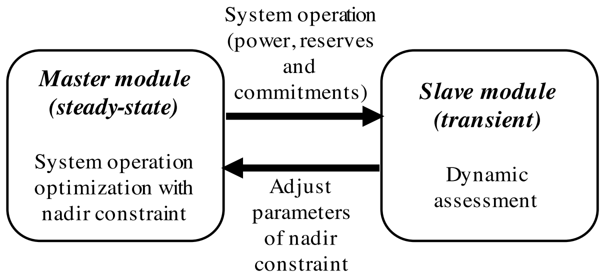

Fig. 1. Overview of the proposed model.

Second, the model is industry-friendly as the parameters used to optimize system operation are accurately tuned by a detailed simulation model (e.g., Power Factory DIgSILENT).

The contributions in our proposal are outlined below:

(1) Propose, design, and implement a sequential optimization-simulation model to operate power systems optimally, while ensuring adequate frequency nadir when occurs the disconnection of the largest online generating unit.
(2) Demonstrate the advantages of committing the units with the best governor's dynamic response, which can only be undertaken if the model appropriately recognizes the unique responses from every unit according to the faced operating condition.
(3) Compare our frequency nadir-constrained model against an alternative inertia-constrained model, demonstrating that ensuring minimum inertia levels can be significantly inefficient, particularly in the presence of large amounts of CGTs.
(4) Demonstrate the advantages of committing frequency-responsive units rather than inertia-heavy units, particularly in light of the high penetration of CGTs.

This paper is structured as follows. Section 2 presents the proposed optimization-simulation model that ensures an adequate frequency response. Section 3 presents and discusses the main results obtained. Finally, Section 4 summarizes the main conclusions of this work.

2. The optimization-simulation model

2.1. Overview

We propose a novel two-stage approach for optimizing power system operations considering realistic frequency excursions and constraining the frequency nadir. The first stage corresponds to a mixed-integer linear program representing the economic dispatch problem with a set of extra constraints, ensuring frequency stability, whose parameters are iteratively adjusted through a Gauss–Seidel approach [16]. The second stage corresponds to a simulation model (Power Factory DIgSILENT), which iteratively adjusts and updates the parameters of the first stage's constraints. The adjusted parameters characterize the response of every generating unit to the most significant power imbalance at a particular operating point. The iterative process stops when the parameters in the optimization model (first stage) properly represent the system response observed in the simulation model (second stage). The proposal includes a detailed dynamic response of each SG. The sequential approach is presented in Fig. 1.
In the following subsections, we present the main aspects of the proposed model. In Section 2.2, we explain the master (optimization) module. Section 2.3 presents the nadir constraint that is added in the system operation optimization. Section 2.4 presents the iterative Gauss–Seidel algorithm. Finally, in Section 2.5, an alternative inertia-constrained approach is presented for comparison purposes.

2.2. The classic system operation model (without the frequency nadir constraint)

The master module of the proposed methodology optimizes the system operation in terms of power, reserves, and commitment. The master module may correspond to any system operation optimization model with explicit reserves requirements, for instance: optimal power flow (OPF), security-constrained economic dispatch (SCED), security-constrained unit commitment (SCUC). This is the case since our proposed approach can be applied to any system operation optimization problem with explicit reserves requirements (where the post-contingency states are not modeled). For simplicity, we applied our proposition on a SCED that determines the optimal dispatches of energy and reserves (and the units' commitment on/off statuses) like that in [17]. The SCED optimization model is presented below:

$$\min_{P_i,R_i,Y_i,f_k,\theta_b} \sum_{i\in I} c_i\left(P_i, R_i\right) \tag{1}$$

subject to:

$$\sum_{i\in I_b} P_i + \sum_{k\in K|to(k)=b} f_k - \sum_{k\in K|fr(k)=b} f_k = D_b \quad \forall\, b\in B \tag{2}$$

$$f_k = \frac{1}{x_k}(\theta_{fr(k)} - \theta_{to(k)}) \qquad \forall\, k\in K \tag{3}$$

$$-\bar{f}_k \le f_k \le \bar{f}_k \qquad \forall k\in K \tag{4}$$

$$P_i + R_i \le \bar{P}_i \cdot Y_i \qquad \forall i\in I \tag{5}$$

$$P_i + R_i \ge \underline{P_i} \cdot Y_i \qquad \forall i\in I \tag{6}$$

$$0 \le R_i \le \bar{R}_i \cdot Y_i \qquad \forall i\in I \tag{7}$$

$$\sum_{i\in I|i\neq l} R_i \ge P_l \qquad \forall i\in I \tag{8}$$

The objective function (1) minimizes the operating costs, in this case, the fuel cost associated with the power generation, and reserves. Eq. (2) ensures the generation-demand balance at each node of the system. The DC power flow between two nodes is presented in (3), bounded by the corresponding network capacity limits by (4). Eqs. (5) and (6) impose bounds on the power generating units, including operating reserves. Eq. (7) impose bounds on operating reserves from each generating unit. The commitment binary variable is denoted as Y_i. Finally, Eq. (8) defines the necessary spinning reserve when the disconnection of the largest online generating unit (P_l) occurs. In the following sections, the formulation is complemented to limit the frequency nadir.

2.3. Adding the frequency nadir constraint

This subsection presents the extra constraint added in the master module to limit the frequency nadir. The constraint determines the reserve requirement by each SG to arrest the excursion of frequency after P_l occurs. The constraint also considers the governor behavior through the governor ramp rate response capability (ρ_i). Next, we derive the constraint in a step-by-step approach, starting from the swing Eq. (9).

$$\frac{df(t)}{dt} = \frac{P_m(t) - P_e(t)}{M_H} \tag{9}$$

In (9), $P_m(t) - P_e(t)$ represents the power imbalance, and M_H represents the system inertia after the loss of P_l. M_H is defined by the summation of the inertia coefficients (M_i) of the online generating units. M_H is calculated according to Eq. (10). Note that M_H is dependent on the commitment variable Y_i.

$$M_H = \sum_{i\in I} M_i \cdot Y_i \qquad \forall i\in I; i\neq l \tag{10}$$

From the swing equation, we can derive an equation that incorporates ramp rate ρ_{Nadir} of all SG, which can be stated in Eq. (11).

$$\rho_{Nadir} = \frac{\frac{1}{2} P_l^2}{M_H \cdot (f_0 - f_{Nadir}) - P_l \cdot t_F} \tag{11}$$

where f_0 represents the nominal frequency of the system. The frequency nadir (f_{Nadir}) defines the minimum frequency value, which relates to the remaining system inertia M_H in the post-contingency state.

In addition, the governors have a deadband zone. In this zone, the action control is null. The deadband is related to the first instants after the contingency occurs. Therefore there is a dead time (t_F) related to deadband frequency (f_{db}). t_F is calculated by Eq. (12):

$$t_F = \frac{M_H}{P_l} \cdot f_{db} \tag{12}$$

Using (11) and (12), it is possible to establish the minimum ramping capability (ρ_{min}) that ensures $f_{Nadir} \geq f_{min}$. ρ_{min} can be stated using Eq. (13).

$$\rho_{min} = \frac{\frac{1}{2} P_l^2}{M_H \cdot (f_0 - f_{min} - f_{db})} \tag{13}$$

Finally, considering (8) we can define (14):

$$R_i \leq 2 \cdot \rho_i \frac{M_H \cdot (f_0 - f_{min} - f_{db})}{P_l} \quad \forall i \in I; i \neq l \tag{14}$$

Therefore, the system operation with nadir constraint is defined by adding (10) and (14) into the formulation presented in 2.2 to ensure adequate f_{Nadir}. Eq. (14) shows the dependency among ρ_i, M_H and P_l. Also, f_0, f_{min}, f_{db} are known parameters [18]. For further details about the mathematical expressions, see Appendix. Notice that Eq. (14) is a non-linear constraint because ρ_i is not a constant. This is a key point in our work since the vast majority of the published models so far assumes ρ_i as a constant, transforming a non-linear constraint into a linear constraint. Additionally, the governor ramp rate (ρ_i) is unique for each SG unit, and it is of great significance in the dynamic response of the system.

Let us assume that ρ_i can be approximated using the expression (15), where $t_{f_{Nadir}}$ and P_{Nadir} are obtained at the point of the minimum value of frequency (f_{Nadir}). t_f is the time when the contingency occurs, and P_f is the mechanical power of the generating unit when the contingency occurs (right before).

$$\rho = \Delta P / \Delta t = (P_{Nadir} - P_f)/(t_{f_{Nadir}} - t_f) \tag{15}$$

For example, Fig. 2 shows the governor ramp rate of a unit for two different operating points.[1] As observed, ρ_i significantly changes according to the operating point. The case step response 1 (SR1) shows a mechanical power equal to 0.94 p.u., when f_{Nadir} occurs. Using Eq. (15), the value of ρ_i can be calculated, resulting equal to 0.10 p.u./s. In step response 2 (SR2), using the same equation, ρ_i results equal to 0.045 p.u./s. Notice also that the steady-state conditions are different for both responses (0.6 p.u. and 0.8 p.u.). This example highlights the importance of capturing these differences when determining power system operation.

Notice we use the mechanical power signal, which is a smother signal than that of the electrical power. Hence, there are further oscillations in the electrical power signal (particularly when the load depends on voltage), which we ignore in the calculation of ρ_{min}. Nevertheless, this is a common assumption, resulting in a more straightforward estimation of ρ_{min} [19].

[1] The dynamic responses were obtained from a dynamic simulation (islanded step response).

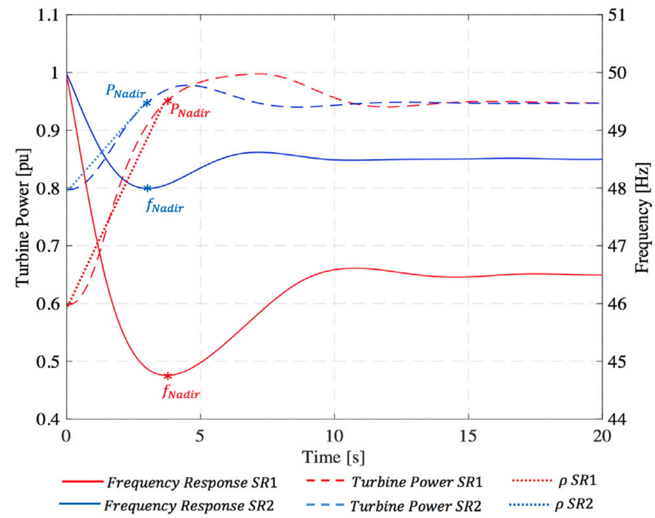

Fig. 2. Governor model step-response assessed in two operating points.

2.4. Solution algorithm: Gauss–Seidel iterations

The proposed algorithm to solve the sequential master–slave approach is presented in Fig. 3. The proposed algorithm is based on a Gauss–Seidel method, allowing to tackle the non-linear nadir constraint in the system operation optimization. Thus, ρ_i for each SG unit in Eq. (14) is adjusted through an iterative process. The algorithm is divided into five steps.

Step 1 — System operation optimization without nadir constraint: In this step, any system operation optimization model might be implemented without considering a nadir constraint (OPF, SCED, SCUC) to minimize the system operational cost with explicit requirements of reserves. Notice step 1 is the initialization process (see Fig. 3).

Step 2 — Dynamic assessment: The results obtained in the previous stage are then validated through time-domain simulations (TDS), considering a detailed dynamic model of the system. The main idea is to detect hazard situations from a frequency stability perspective when the disconnection of the largest online generating unit P_l is simulated. If the system frequency drops below a predefined minimum threshold ($f_{Nadir} \geq f_{min}$), under frequency load shedding schemes (UFLSS) are activated, and thus, the process continues with the next step. Otherwise, the process ends. According to the proposed methodology, if the criterion $f_{Nadir} \geq f_{min}$ is fulfilled, using the SCED without nadir constraint, this is the optimal solution and the process ends. Otherwise, the SCED with nadir constraint formulation (step 3) must be solved (iterative process).

Step 3 — System operation optimization with nadir constraint: In this step, SCED with nadir constraint is run considering the ρ_i values obtained from each SG dispatched in step 2. A step response simulation for every SG is performed to obtain the initial values of ρ_i that were not considered in the dispatch solution in the previous step. The power injected by every SG of the system is obtained and then used in the next step.

Step 4 — Dynamic assessment: The dispatch obtained from step 3 is dynamically evaluated for the disconnection of the largest (online) generator through a TDS. If $f_{Nadir} \geq f_{min}$, the solution obtained in the previous step ensures adequate frequency performance (avoiding the activation of UFLSS), and thus the iterative process ends. Otherwise, the process continues to the next step.

Step 5 Adjustment of ρ_i: In this step, the value of ρ_i of every SG is adjusted based on their dynamic response obtained from step 4 and using Eq. (15). The new values of ρ_i are used in the next iteration. The whole iterative process ends when $f_{Nadir} \geq f_{min}$.

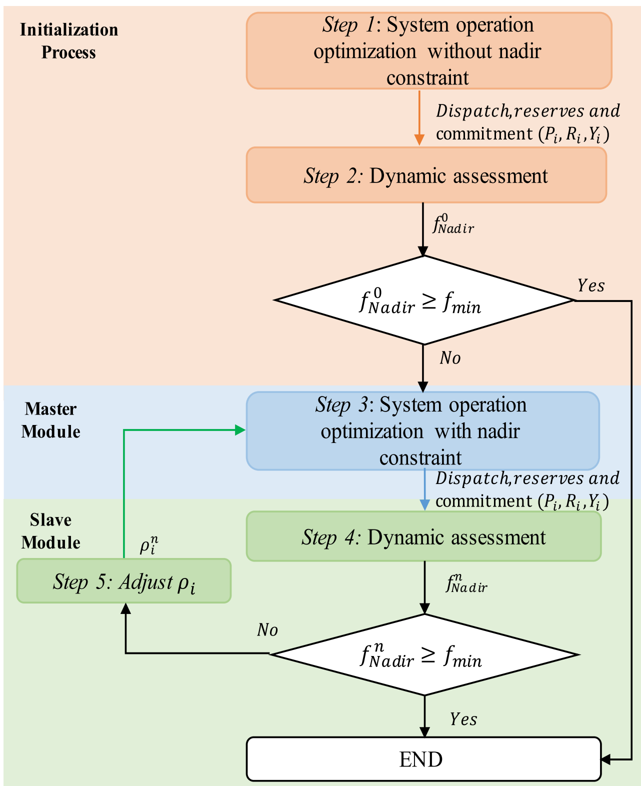

Fig. 3. Diagram of the algorithm (n is the number of the iteration).

Table 1
System data.

Unit	Num. of units	Var. Cost USD/MWh	Unit type	Gover. Model	Inst. Cap. MW	$\overline{R_i}$ MW	Inertia s
U12	5	228	Oil/Steam	IEEEG1	12	3.6	2.8
U20	4	228	Oil/CT	IEEEG1	20	6	2.8
U50	6	0	WT	–	50	0	0
U75	4	0	WT	–	75	0	0
U100	9	228	Oil/Steam	TGOV1	100	30	2.8
U155	12	24	Hydro	Hydro	155	46.5	3
U197	3	228	Oil/Steam	TGOV1	197	59.1	2.8

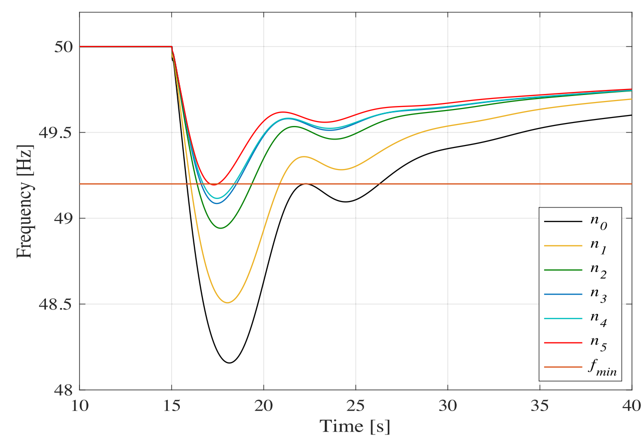

Fig. 4. System frequency response for various iterations (n_0 to n_5). The threshold f_{min} is also displayed.

2.5. Alternative inertia-constrained optimization model

An alternative inertia-constrained approach is proposed, where a minimum level of inertia is imposed as a constraint in the system operation optimization problem presented in Section 2.2. Eq. (16) shows the inertia constraint, where T_H is the specific requirement of inertia. In the alternative approach, Eq. (16) is added to the formulation (1)–(8).

$$\sum_{i \in I} M_i \cdot Y_i \geq T_H \qquad \forall i \in I; i \neq l \tag{16}$$

We present this formulation for comparison purposes as, apart from proposing a new model, we seek to discuss the differences between constraining frequency nadir versus constraining inertia levels.

3. Results and discussion

3.1. Input data

Table 1 summarizes the features of each generating unit of the test system under study. The SG installed capacity and inertia values are based on the IEEE reliability test system (IEEE One area RTS-96) [20]. Importantly, the models are based on “Dynamic Models for Turbine Governors in Power System Studies” [21]. To fulfill the criterion $f_{Nadir} \geq f_{min}$, we assume that: the dead-band frequency (f_{db}) is 0.05 Hz, the minimum permissible frequency (f_{min}) is 49.2 Hz, and the nominal frequency (f_0) is 50 Hz. In addition, extra wind turbine generating units (WT) are installed in buses: 1 (150 MW), 2 (150 MW), and 22 (300 MW).

The master module is implemented in FICO Xpress Optimization Suite software [22], and the dynamic simulation is performed in DigSILENT Power Factory software [23]. The simulations were performed in a computer with 1 Intel Core i7 4890HQ (4 cores) and 16 GB of RAM. The computational performance during the simulations depends on three main aspects: (i) the specific system operation optimization model selected, (ii) the power system size and its complexity (penetration level of CGTs, dynamic models of the power system components, the complexity of SG plant models, among others), and (iii) the computational capacity to solve the optimization problem and to perform the time-domain simulations. For the system under study, one run (including all iterations until the model converges) of a case study shown next lasts 240 s on average.

3.2. Results

Fig. 4 shows the excursion of frequency for each iteration of the algorithm. In the first iteration, the f_{Nadir} is 48.16 Hz, the iterative process ends when the frequency requirements are met. These results highlight the importance of a correct inertial response representation and an appropriate model to recognize detailed frequency excursion. Note that in each iteration, an optimization model is solved with a linear frequency nadir constraint and a credible set of values of ρ_i. This demonstrates that a single linear optimization problem might not appropriately capture inertial responses. Our approach exploits sequential linear problems to tackle this issue, which clearly improves the solution.

An important consequence of improving the frequency response is the increased operating cost due to increased reserves. This operating cost is necessary to meet the frequency nadir constraint. Table 2 shows the operating cost in every iteration.

Fig. 5 shows the frequency responses of both the frequency nadir-constrained and the inertia-constrained solutions. To obtain the inertia level required by the inertia-constrained model, we calculate the inertial level of the frequency nadir-constrained solution. Thus, we can ensure that both responses in Fig. 5 contain the same levels of inertia. Despite this, the frequency responses are different. In fact, the solution with the explicit inertia requirement presents a worse performance

Table 2
Operating cost and f_{Nadir} values.

Iteration n	f_{Nadir} [Hz]	Oper. Cost [USD]
0	48.16	5810
1	48.51	6720
2	48.94	12 780
3	49.09	17 340
4	49.10	19 530
5	49.12	20 630
6	49.20	21 900

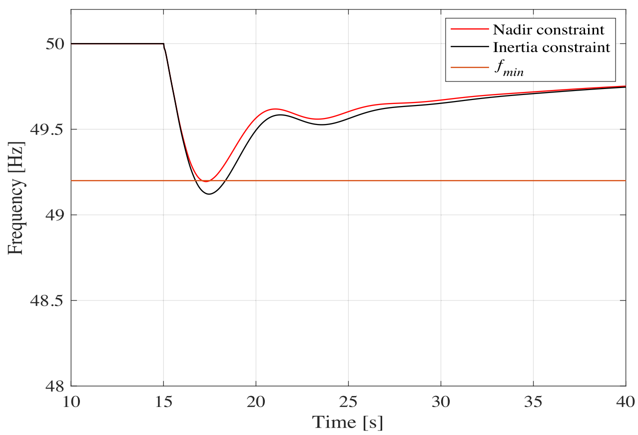

Fig. 5. Frequency response of the solution with nadir constraint and the solution with inertia constraint.

Table 3
Operating cost and f_{Nadir} values for system operation with nadir constraint vs. system operation with inertia constraint.

Approach	f_{Nadir} [Hz]	Oper. Cost [USD]
Nadir constraint	49.20	21 900
Inertia constraint	49.12	21 900

in terms of frequency stability. This highlights the risks associated with focusing on inertia levels only rather than on the overall system frequency stability.

Interestingly, Table 3 shows that the frequency nadir-constrained solution is not costly compared to the inertia-constrained solution, despite the fact that the performance of the former is better and, therefore, more secure.

The improved performance of the frequency nadir-constrained solution can be better understood by studying the unit commitments shown in Fig. 6. Expectedly, Fig. 6 shows that the inertia-constrained solution considers a higher number of SGs committed. Despite this, this solution presents a worse dynamic performance. As our model is able to recognize the units with the best governor's dynamic behavior, it commits more 100-MW units that feature a much faster response against the largest loss of power.

As a final remark, it is important to highlight that the differences observed in Fig. 6 can be exacerbated significantly with increased levels of renewable generation. For instance, Fig. 7 shows the solutions of the frequency nadir-constrained and inertia-constrained models when we force not to curtail wind power (both solutions feature the same inertia levels). This demonstrates that increasing amounts of renewables may be treated more efficiently through frequency nadir-constrained models rather than through inertia-constrained models.

4. Conclusions

We propose a sequential optimization-simulation model to optimize system operation with nadir considerations via simulation of detailed

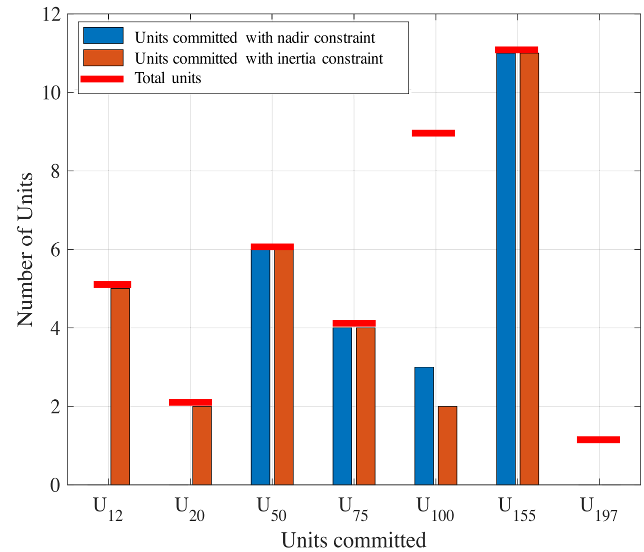

Fig. 6. Unit commitment of the solutions with nadir and inertia constraints.

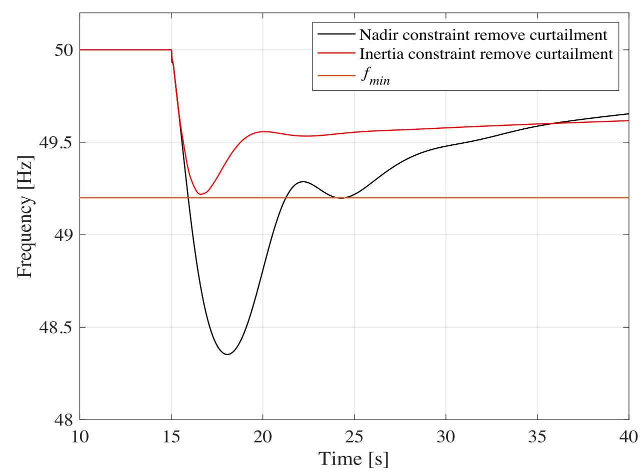

Fig. 7. Frequency response for the solution with nadir constraint and with inertia constraint, eliminating wind curtailments.

system dynamic responses. Through simulations, the model can recognize the precise governor's dynamic response of each unit (that depends on the operating condition of the unit). This information is given to the optimization stage in order to find the optimal power system operation that ensures reliable levels of frequency nadir when facing the largest loss of power. Since our approach can be applied by using actual industry-based tools (a system operation optimization tool and a dynamic simulation tool) and relies on a well-understood Gauss–Seidel method, we believe that our proposition can be more easily accepted and implemented for real-world applications.

We demonstrate the advantage of recognizing and committing the units with the best system dynamic responses through several case studies. We compare our frequency nadir-constrained solution against an alternative inertia-constrained solution, demonstrating that ensuring minimum inertia levels can be inefficient, particularly under the high penetration of CGTs. These results are relevant for policymakers, regulators and operators, who attempt to find the best way to integrate more and more renewables without affecting system stability.

One interesting topic for further work is including the emulated inertial response from CGTs to demonstrate its applicability, particularly in scenarios with high penetration of these technologies. Another interesting topic for further work is including system damping, which

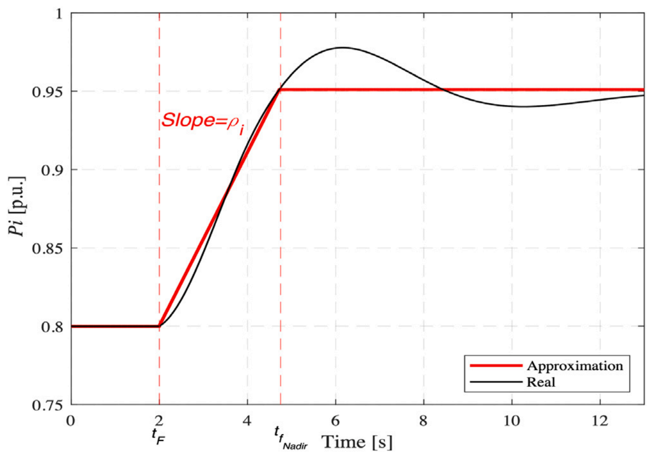

Fig. A.1. Governor ramp rate (ρ_i) approximation.

may change the swing equation and the approximations made when adding the frequency nadir constraint. Also, adding RoCoF constraints in the optimization model is an interesting future research avenue to complement the proposed frequency nadir constraint. A final but crucial interesting topic for further work is designing the actual implementation of these concepts and models in a market environment, where ancillary services need to be defined and remunerated, and their costs need to be allocated among various market participants.

CRediT authorship contribution statement

Diego Ortiz-Villalba: Conception and design of study, Acquisition of data, Analysis and/or interpretation of data, Writing – original draft. **Jacqueline Llanos:** Conception and design of study, Acquisition of data, Writing – original draft. **Yanira Muñoz-Jadan:** Conception and design of study, Acquisition of data, Writing – original draft. **Rodrigo Moreno:** Conception and design of study, Analysis and/or interpretation of data, Writing – original draft, Writing – review & editing. **Claudia Rahmann:** Writing – review & editing. **Bikash C. Pal:** Writing – review & editing.

Declaration of competing interest

The authors declare that they have no known competing financial interests or personal relationships that could have appeared to influence the work reported in this paper.

Acknowledgments

The authors gratefully acknowledge the financial support from ANID, Chile, through grants CONICYT/63140112, PIA/APOYO AFB1-80003 (Instituto Sistemas Complejos de Ingenieria ISCI), and Fondecyt /1181928. All authors approved the final version of the manuscript.

Appendix. Approximations of ρ_{Nadir}

After a contingency, SGs increase their power output $P_i(t)$ in response. Following [24], the ramp rate (ρ_i) can be approximated as shown in Fig. A.1.

The approximation assumes that there is a dead time t_F that is a feature of governor response. $t_{f_{Nadir}}$ can be calculated considering the swing Eq. (9) and the simplification shown in Fig. A.1, as follows:

$$\frac{df(t)}{dt} = 0 \Rightarrow \rho_{Nadir} \cdot (t_{f_{Nadir}} - t_F) = P_l$$
$$\Rightarrow t_{f_{Nadir}} = \frac{P_l}{\rho_{Nadir}} + t_F \tag{A.1}$$

This considers that frequency derivative must be zero at the $t_{f_{Nadir}}$. Replacing (A.1) in (9), the value of f_{Nadir} can be obtained as follows:

$$\int_0^{t_{f_{Nadir}}} \frac{df(t)}{dt} dt = f(t_{f_{Nadir}}) - f(0) = f_{Nadir} - f_0$$
$$\Rightarrow f_{Nadir} - f_0 = \frac{1}{M_H} \cdot \left(\int_0^{t_F} -P_l dt \right) + \frac{1}{M_H} \cdot \left(\int_{t_F}^{t_{f_{Nadir}}} (\rho_{Nadir} \cdot t - P_l) dt \right) \tag{A.2}$$

Notice that the above integral is divided into two parts, and the bounds of the first part have been re-arranged so that the lower bound is zero. Hence, the value of the f_{Nadir} is determined by:

$$f_{Nadir} - f_0 = -\frac{1}{M_H} \cdot \left(\frac{P_l^2}{2\rho_{Nadir}} + P_l \cdot t_F \right) \tag{A.3}$$

Re-arranging (A.3), ρ_{Nadir} can be determined by:

$$\rho_{Nadir} = \frac{\frac{1}{2} P_l^2}{M_H \cdot (f_0 - f_{Nadir}) - P_l \cdot t_F} \tag{A.4}$$

References

[1] NERC, Reliability Guideline Primary Frequency Control, tech. rep., NERC, 2016.
[2] P.J. Vogler-Finck, W.-G. Früh, Evolution of primary frequency control requirements in Great Britain with increasing wind generation, Int. J. Electr. Power Energy Syst. 73 (2015) 377–388.
[3] H. Bevrani, Robust Power System Frequency Control, Vol. 85, Springer, 2009.
[4] J. Eto, et al., Use of Frequency Response Metrics to Assess the Planning and Operating Requirements for Reliable Integration of Variable Renewable Generation, tech. rep., Ernest Orlando Lawrence Berkeley National Laboratory, 2011.
[5] R. Pearmine, Y. Song, A. Chebbo, Influence of wind turbine behaviour on the primary frequency control of the British transmission grid, IET Renew. Power Gener. 1 (2) (2007) 142–150.
[6] P. Gardner, H. Snodin, A. Higgins, S. McGoldrick, The Impacts of Increased Levels of Wind Penetration on the Electricity Systems of the Republic of Ireland and Northern Ireland: Final Report, Garrad Hassan and Partners Limited, 2003, pp. 1–39.
[7] E. Vittal, A Static Analysis of Maximum Wind Penetration in Iowa and a Dynamic Assessment of Frequency Response in Wind Turbine Types, Iowa State University, 2008.
[8] A. Inzunza, R. Moreno, A. Bernales, H. Rudnick, CVaR constrained planning of renewable generation with consideration of system inertial response, reserve services and demand participation, Energy Econ. 59 (2016) 104–117.
[9] K. Komasatid, S. Jiriwibhakorn, Flexibility and frequency security enhancement to generation expansion planning framework, in: 2019 IEEE PES GTD Grand International Conference and Exposition Asia (GTD Asia), IEEE, 2019, pp. 762–767.
[10] L. Badesa, F. Teng, G. Strbac, Simultaneous scheduling of multiple frequency services in stochastic unit commitment, IEEE Trans. Power Syst. 34 (5) (2019) 3858–3868.
[11] H. Ahmadi, H. Ghasemi, Security-constrained unit commitment with linearized system frequency limit constraints, IEEE Trans. Power Syst. 29 (4) (2014) 1536–1545.
[12] M. Brito, E. Gil, I. Calle, Unit commitment with primary frequency control requirements for low-inertia systems, in: 2018 IEEE Power & Energy Society General Meeting (PESGM), IEEE, 2018, pp. 1–5.
[13] H. Gu, R. Yan, T.K. Saha, E. Muljadi, System strength and inertia constrained optimal generator dispatch under high renewable penetration, IEEE Trans. Sustain. Energy 11 (4) (2019) 2392–2406.
[14] Z. Zhang, E. Du, G. Zhu, N. Zhang, C. Kang, M. Qian, J.P. Catalão, Modeling frequency response dynamics in power system scheduling, Electr. Power Syst. Res. 189 (2020) 106549.
[15] G. Zhang, J. McCalley, Optimal power flow with primary and secondary frequency constraint, in: 2014 North American Power Symposium (NAPS), IEEE, 2014, pp. 1–6.
[16] H. Saadat, Power System Analysis, Vol. 1, second ed., McGraw-Hill Higher Education, 2009.
[17] J.M. Arroyo, F.D. Galiana, Energy and reserve pricing in security and network-constrained electricity markets, IEEE Trans. Power Syst. 20 (2) (2005) 634–643.
[18] H. Chavez, R. Baldick, S. Sharma, Governor rate-constrained OPF for primary frequency control adequacy, IEEE Trans. Power Syst. 29 (3) (2014) 1473–1480.
[19] D. Zografos, Power System Inertia Estimation and Frequency Response Assessment (Ph.D. thesis), KTH Royal Institute of Technology, 2019.

[20] C. Grigg, P. Wong, P. Albrecht, R. Allan, M. Bhavaraju, R. Billinton, Q. Chen, C. Fong, S. Haddad, S. Kuruganty, et al., The IEEE reliability test system-1996. A report prepared by the reliability test system task force of the application of probability methods subcommittee, IEEE Trans. Power Syst. 14 (3) (1999) 1010–1020.
[21] P. Pourbeik, et al., Dynamic models for turbine-governors in power system studies, in: IEEE Task Force on Turbine-Governor Modeling, no. 2013, 2013.
[22] FICO xpress optimization suite, 2021, avaliable: http://www.fico.com/en/products/.
[23] Power factory DIgSILENT, 2021, avaliable: https://www.digsilent.de/en/.
[24] H. Chavez, R. Baldick, Inertia and governor ramp rate constrained economic dispatch to assess primary frequency response adequacy, in: Proc. Int. Conf. Renewable Energies and Power Quality, Citeseer, 2012, pp. 1–6.